



Oxygen Balance for Small Organisms: an Analytical Model

J. L. W. GIELEN

Department of Mathematical and Statistical Methods,
Biometris, Wageningen University,
Dreijenlaan 4,
6703 AH Wageningen,
The Netherlands
E-mail: jo.gielen@mat.dpw.wag-ur.nl

S. KRANENBARG

Experimental Zoology Group, WIAS,
Wageningen University,
Marijkeweg 40,
6709 PG Wageningen,
The Netherlands
E-mail: sander.kranenbarg@morf.edc.wag-ur.nl

An analytical model is developed that describes oxygen transport and oxygen consumption for small biological structures without a circulatory system. Oxygen inside the organism is transported by diffusion alone. Oxygen transfer towards the organism is retarded by a thin static fluid film at the surface of the organism. The thickness of this film models the outward water conditions, which may range from completely stagnant water conditions to so-called well-stirred water conditions. Oxygen consumption is concentration-independent above a specified threshold concentration (regulator behaviour) and is proportional to the oxygen concentration below this threshold (conformer behaviour). The model takes into account shape and size of the organism and predicts the transition from (pure) regulator behaviour to (pure) conformer behaviour, as well as the mean oxygen consumption rate. Thereby the model facilitates a proper analysis of the physical constraints set on shape and size of organisms without an active internal oxygen transport mechanism. This analysis is carried out in some detail for six characteristic shapes (infinite sheet, cylinder and beam; finite cylinder, sphere and block). In a well-stirred external medium, a flattened shape appears to be the most favourable for oxygen supply, while a compact shape (cube) is more favourable if the external medium is nearly stagnant. The theoretical framework is applied to oxygen consumption data of eight teleost embryos. This reveals relative insensitivity to external flow conditions in some species (e.g., winter flounder, herring), while others appear to rely on external stirring for a proper oxygen supply (e.g., largemouth bass). Interestingly, largemouth bass is the only species in our analysis that exhibits 'fin-fanning'.

© 2002 Society for Mathematical Biology

1. INTRODUCTION

Molecular diffusion is an important mechanism by which oxygen is transported to respiring biological structures. However, molecular diffusion is only efficient over relatively short distances, or as formulated by Krogh (1941): ‘diffusion alone can provide sufficient oxygen only to organisms of 1mm diameter or less’. Molecular diffusion thus poses a physical constraint on the size and shape of an organism that does not (yet) have an additional way of oxygen transport (Graham, 1988). Mathematical models of oxygen transport may serve to gain quantitative insight in these constraints and the parameters involved.

Models of oxygen flow to biological structures date back to Warburg (1923), Fenn (1927) and Harvey (1928), who modelled steady state diffusion of oxygen from a well-stirred solution to liver slices, frog nerves and bacteria, respectively. Warburg (1923) and Fenn (1927) calculated maximum diffusion distances, while Harvey (1928) calculated a minimum surface oxygen tension for the bacterium to maintain an adequate respiration. Gerard (1931) extended this model for a varying diffusion constant and oxygen consumption pattern in the sphere. These authors modelled steady state diffusion of oxygen from a well-stirred solution into a one-dimensional (1D) structure (only the radius is a variable shape-factor) under the assumption that volume-specific oxygen consumption is independent of oxygen concentration (regulator behaviour).

Strathmann and Chaffee (1984) elaborated on these models to formulate size constraints for invertebrate egg masses, while Lee and Strathmann (1998) included the depletion of oxygen in a boundary layer around a spherical egg or egg-mass. Seymour and Bradford (1987) modelled the effect of an impeding gelatinous capsule on the oxygen delivery to a spherical egg and predicted maximum sizes of amphibian eggs and egg capsules.

Daykin (1965) and Wickett (1975) applied mass transfer theory to oxygen transport in respiring fish eggs. They predicted the bulk flow velocity required for proper egg development. Kranenborg *et al.* (2001) employed mass transfer theory to predict maximum size and optimal shape of small organisms for any bulk flow velocity.

The assumption of concentration-independent consumption was alleviated by Byatt-Smith *et al.* (1991) in their nonsteady-state models of oxygen diffusion to mouse and human preimplantation embryos in the absence of stirring. They modelled the volume-specific oxygen consumption of the embryos both as being independent of the oxygen concentration (regulator) and as being directly proportional to the oxygen concentration (conformer), though both models were mutually exclusive.

This short historical sketch shows three important aspects in models of oxygen transport to small organisms: shape and size of the organism, oxygen consumption pattern of the organism and flow condition of the medium around the organism. In the present paper we incorporate all these aspects of the oxygen transport pro-

blem in one analytical model. We represent the actual organism by a region G in space, which determines the size and shape of the organism. Analytical solutions of the resulting formalism for some special 1D cases (infinite sheet, infinite cylinder, sphere) and some higher-dimensional cases (infinite beam, rectangular parallelepiped and finite cylinder) are included. The oxygen consumption behaviour of our model organism is, in essence, a mixed form of conformer behaviour (at low oxygen concentrations) and regulator behaviour (at higher oxygen concentrations), as is generally found by experiment [e.g., Longmuir (1957)]. Pure regulator and pure conformer behaviour are included as limiting cases in our model. Convective oxygen transport to the organism is incorporated in our model by the introduction of a thin static fluid film around the organism, through which oxygen is transported (Carslaw and Jaeger, 1959; Rosen, 1952). The thickness of this layer will be translated in a transport coefficient k_{eff} . A well-stirred external medium is represented by a layer of (almost) zero thickness, while more or less stagnant water conditions are represented by a positive thickness of the encapsulating layer, and hence by a finite value for k_{eff} .

With the inclusion of these aspects in our model we are able to make a proper analysis of the constraint oxygen transport sets on the size and shape of organisms that do not have an active internal oxygen transport mechanism.

2. THE MODEL

2.1. Preliminaries. We wish to describe the stationary oxygen concentration inside a small organism surrounded by water as a function of (1) the shape and size of the organism, (2) the oxygen consumption pattern the organism exhibits, (3) the outside conditions the organism experiences. The organism is modelled as a region G in 3-dimensional (3D) space; the surface of the organism is denoted as ∂G . The oxygen concentration inside the organism at place \vec{x} and time t is described by the function $u(\vec{x}, t)$, with $\vec{x} \in G$ and $t > 0$. Then the stationary (equilibrium) oxygen concentration inside the organism is given by $u(\vec{x}) = u(\vec{x}, \infty)$, with $\vec{x} \in G$.

Oxygen inside the organism is transported by diffusion; the (constant) diffusion coefficient is denoted as D . It is assumed that barriers to oxygen diffusion and possible movements of the protoplasm or interstitial fluid can be adequately accounted for in the value of this diffusion coefficient [e.g., Desaulniers *et al.* (1996), Dowse *et al.* (2000) and Krogh (1919)]. These authors show that the diffusion coefficient of oxygen in animal tissue is about three times smaller than its value in water.

Furthermore oxygen will be consumed inside the organism. We suppose that the oxygen consumption rate F at place \vec{x} and time t is in the following way a function of the oxygen concentration $u = u(\vec{x}, t)$:

$$F(u) = \begin{cases} m & \text{if } u \geq C_0, \\ mu/C_0 & \text{if } u \leq C_0. \end{cases} \quad (2.1)$$

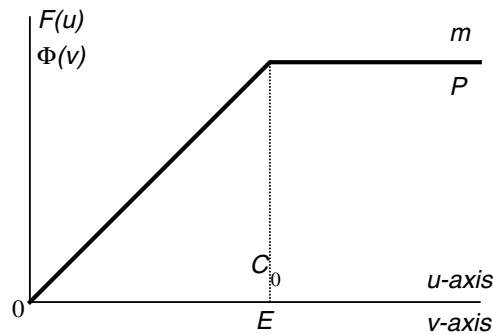


Figure 1. The oxygen consumption rate $F(u)$ of the organism (dimensionless: $\Phi(v)$). For $u < C_0$ (dimensionless: $v < E$) there is conformer behaviour; for $u > C_0$ (dimensionless: $v > E$) there is regulator behaviour. The maximum consumption rate equals m (dimensionless: P).

This assumption implies a uniform oxygen consumption throughout the embryo, while in reality oxygen is consumed by a large number of point sinks, i.e., the mitochondria. To reduce mathematical complexity, however, we assume the effect of all these point sinks on the final oxygen distribution to be the same as a uniform oxygen consumption. Preliminary measurements of the oxygen concentration inside a zebrafish (*Danio rerio*) embryo *in vivo* indeed supports this assumption.

The threshold concentration C_0 marks the transition between so-called regulator behaviour and conformer behaviour. We say the organism exhibits at place \vec{x} and time t regulator behaviour if $u(\vec{x}, t) \geq C_0$. This means that the oxygen concentration is locally sufficiently high for the organism to consume all the oxygen it can use. The consumption rate at such a point will therefore be at its maximum value m . If $u(\vec{x}, t) < C_0$ we say the organism exhibits at place \vec{x} and time t conformer behaviour. This means that the oxygen concentration is locally too low to fulfil all the needs of the organism. Accordingly it scales down its consumption to a (constant) fraction of the available oxygen, see Fig. 1. Of course the organism as a whole can be in a mixed state: then there is only a lack of oxygen and thus conformer behaviour in (typically) some small interior part of G , while the outer parts of G still exhibit regulator behaviour. We designate an organism as a pure regulator (conformer) if it exhibits regulator (conformer) behaviour in all points of G .

It can be expected that the transition from pure regulator behaviour to mixed case behaviour triggers certain biological modifications in the organism, for instance, the onset of the formation of bloodvessels in the oxygen deprived region. Also the transition from mixed case behaviour to pure conformer behaviour is interesting from a biological point of view: then the organism as a whole experiences oxygen shortage, which may eventually lead to the complete shut-down of certain biological functions inside the organism (Padilla and Roth, 2001). For these reasons we will pay special attention to the parameter values for which these transitions occur.

In general the free water oxygen concentration C_∞ does not equal the oxygen concentration at the surface of the organism. The first reason for this phenomenon

stems from the solubility of oxygen in the organism's tissue. With K the (dimensionless) Henry coefficient for oxygen with respect to water and tissue, the oxygen concentration in water directly at the surface ∂G equals $u(\vec{x}, t)/K$. For biological tissue K will generally equal or be close to one. The second reason is found in the formation of a thin static fluid film of water at the surface of the organism (Carslaw and Jaeger, 1959; Rosen, 1952). The average thickness of this layer depends on the water movement around the organism. In more or less stagnant water conditions this film will be relatively thick, while in running water conditions this layer will be practically nonexistent. We suppose that oxygen transport through this layer obeys Fick's first law. This leads to the equation:

$$D \frac{\partial}{\partial \vec{n}} u(\vec{x}, t) = k_{\text{eff}} \left[C_{\infty} - \frac{u(\vec{x}, t)}{K} \right], \quad \text{for } \vec{x} \in \partial G \text{ and } t > 0. \quad (2.2)$$

The so-called mass transfer coefficient $k_{\text{eff}} = D_w/\delta$, where δ represents the (averaged) thickness of the static film and D_w the diffusion coefficient of oxygen in water. In this way k_{eff} delivers a measure for the thickness of the static layer, and thereby for the outward water conditions. Running water conditions can be characterized by the equation:

$$u(\vec{x}, t) = K C_{\infty}, \quad \text{for } \vec{x} \in \partial G \text{ and } t > 0. \quad (2.3)$$

Because for $k_{\text{eff}} \rightarrow \infty$ equation (2.2) transforms into (2.3), we may say that the case $k_{\text{eff}} = \infty$ represents running water conditions. The value of k_{eff} under (completely) stagnant water conditions will be discussed in Section 3.3.

2.2. The model equations. The foregoing considerations lead to the following partial differential equation on G and matching boundary condition on ∂G for the oxygen concentration $u(\vec{x}, t)$:

$$\text{PDE: } \frac{\partial}{\partial t} u(\vec{x}, t) = D \Delta_{\vec{x}} u(\vec{x}, t) - F(u(\vec{x}, t)), \quad \text{for } \vec{x} \in G \text{ and } t > 0; \quad (2.4)$$

$$\text{BC: } D \frac{\partial}{\partial \vec{n}} u(\vec{x}, t) + \frac{k_{\text{eff}}}{K} u(\vec{x}, t) = k_{\text{eff}} C_{\infty}, \quad \text{for } \vec{x} \in \partial G \text{ and } t > 0. \quad (2.5)$$

Since the time scale for diffusion equilibrium is very much smaller than the time scale for growth of the organism, we can safely assume diffusion equilibrium at any stage during a growth process. That is why we are, in this paper, mainly interested in the stationary (equilibrium) solution of equations (2.4) and (2.5), which means that an initial condition is not needed.

At this point we introduce in the following way a characteristic length L for the region G :

$$L = V/A, \quad \text{with} \quad V = \int_G 1 \, d\omega, \quad \text{and} \quad A = \int_{\partial G} 1 \, d\sigma. \quad (2.6)$$

So L equals the volume to surface area ratio of the organism, which is in the present context a meaningful notion indeed, as it represents the volume of respiring tissue to be supplied with oxygen per unit surface area (Kranenborg *et al.*, 2000).

Next we introduce, with the help of this characteristic length L , the following dimensionless parameters:

$$\begin{aligned}\vec{\xi} &= \vec{x}/L, & \text{dimensionless place coordinates;} \\ \tau &= Dt/L^2, & \text{dimensionless time;} \\ v(\vec{\xi}, \tau) &= u(\vec{x}, t)/C_\infty, & \text{dimensionless concentration.}\end{aligned}\quad (2.7)$$

The coordinate transformation $\vec{x} \rightarrow \vec{\xi}$ is a simple contraction with its centre in the origin, and transforms the region G into a unique ‘standard’ region G' with the same shape as G , but with a (dimensionless) volume to surface area ratio equal to one. Note that the (dimensionless) time scale τ obtained on G' depends on the size of G .

With the help of equation (2.7) we deduce in a straightforward way the following dimensionless forms for (2.4) and (2.5):

$$\text{PDE: } \frac{\partial}{\partial \tau} v(\vec{\xi}, \tau) = \Delta_{\vec{\xi}} v(\vec{\xi}, \tau) - \Phi(v(\vec{\xi}, \tau)), \quad \text{for } \vec{\xi} \in G' \text{ and } \tau > 0; \quad (2.8)$$

$$\text{BC: } \frac{\partial}{\partial \vec{n}'} v(\vec{\xi}, \tau) + \frac{Q}{K} v(\vec{\xi}, \tau) = Q, \quad \text{for } \vec{\xi} \in \partial G' \text{ and } \tau > 0. \quad (2.9)$$

Here the dimensionless consumption rate Φ is defined as (see Fig. 1):

$$\Phi(v) = \begin{cases} P & \text{if } v \geq E, \\ Pv/E & \text{if } v \leq E, \end{cases} \quad (2.10)$$

and the dimensionless parameters P , Q and E are given by:

$$\begin{aligned}P &= mL^2/(DC_\infty), & \text{dimensionless maximum consumption rate;} \\ Q &= k_{\text{eff}} L/D, & \text{dimensionless mass transfer coefficient;} \\ E &= C_0/C_\infty, & \text{dimensionless threshold concentration.}\end{aligned}\quad (2.11)$$

In this way we have reduced the parameter set D [$\text{m}^2 \text{s}^{-1}$], m [$\text{kg m}^{-3} \text{s}^{-1}$], C_0 [kg m^{-3}], C_∞ [kg m^{-3}], k_{eff} [m s^{-1}], L [m] and K to the dimensionless parameter set P , Q , E and K ; also the region G is transformed into a matching standard region G' .

As already said before in this paper we are mainly interested in the stationary (equilibrium) state of the organism. From equations (2.8) and (2.9) we infer for the dimensionless equilibrium concentration $v(\vec{\xi}) = v(\vec{\xi}, \infty)$ the following boundary value problem:

$$\text{PDE: } \Delta_{\vec{\xi}} v(\vec{\xi}) - \Phi(v(\vec{\xi})) = 0, \quad \text{for } \vec{\xi} \in G'; \quad (2.12)$$

$$\text{BC: } \frac{\partial}{\partial \vec{n}'} v(\vec{\xi}) + \frac{Q}{K} v(\vec{\xi}) = Q, \quad \text{for } \vec{\xi} \in \partial G'. \quad (2.13)$$

From this equilibrium concentration $v(\vec{\xi})$ on G' we retrieve, with the help of equation (2.7), the original equilibrium concentration $u(\vec{x})$ on G . Now we can divide G into two parts: $G = G_{\text{reg}} \cup G_{\text{conf}}$, with $G_{\text{reg}} = \{\vec{x} \in G \mid u(\vec{x}) \geq C_0\}$ and $G_{\text{conf}} = \{\vec{x} \in G \mid u(\vec{x}) \leq C_0\}$. On G_{reg} the organism exhibits regulator behaviour; and on G_{conf} there is conformer behaviour. Roughly speaking, we expect ‘unimpeded growth’ on G_{reg} and we expect ‘adaptive behaviour’ on G_{conf} .

To exemplify the presented theory, we used the oxygen dynamics data from Kranebarg *et al.* (2000) for eight teleost embryos to calculate the corresponding values of the dimensionless parameters used in this paper. These embryos do not have a circulatory system yet and are therefore dependent on diffusion for their internal oxygen supply. The value of the mass transfer coefficient was chosen to represent a bulk flow velocity ranging from $10^{-4} - 10^{-3} \text{ m s}^{-1}$, which is the minimum convection velocity found in natural situations. For this purpose we used the relation between mass transfer coefficient and bulk flow velocity for a spherical particle given by Clift *et al.* (1978). The value for the threshold concentration was obtained from Longmuir (1957). Both the mass transfer coefficient and the threshold concentration were chosen to be equal for all eight embryos: $k_{\text{eff}} = 3.00 \cdot 10^{-5} \text{ m s}^{-1}$ and $C_0 = 6.40 \cdot 10^{-5} \text{ kg m}^{-3}$. This means $E \approx 0.01$; to be complete: for the (dimensionless) Henry coefficient K the value 1 is chosen. Table 1 shows the result.

2.3. Critical points and mean consumption rate. The equilibrium concentration profile $v(\vec{\xi})$ predicted by (2.12) and (2.13) for an organism of shape G' depends of course on the actual parameter values P , Q , E , and K . Also the minimum and maximum values v_{min} and v_{max} which $v(\vec{\xi})$ takes on G' are functions of these parameters. For a given type G' we define in the associated (four-dimensional) parameter space two so-called critical (hyper-)surfaces S_{reg} and S_{conf} by their respective equations:

$$\begin{aligned} S_{\text{reg}} : \quad v_{\text{min}}(P, Q, E, K) &= E, \\ S_{\text{conf}} : \quad v_{\text{max}}(P, Q, E, K) &= E. \end{aligned} \tag{2.14}$$

The surfaces S_{reg} and S_{conf} divide parameter space in three parts. For $v_{\text{min}}(P, Q, E, K) \geq E$ the organism is a (pure) regulator: $G = G_{\text{reg}}$. For $v_{\text{max}}(P, Q, E, K) \leq E$ the organism is a (pure) conformer: $G = G_{\text{conf}}$. For all other cases the organism is in a mixed state.

If we vary (in some continuous way) the parameters of the model, the result will be a trajectory in parameter space. A point of intersection of such a trajectory with S_{reg} or S_{conf} we call a critical point: in passing one of these surfaces we expect an essential change in the behaviour of the organism.

For instance, it is to be expected that most of the parameters of our model are a function of the ambient temperature T . Thus, for a (slowly) varying temperature T the organism follows a trajectory $\langle P(T), Q(T), E(T), K(T) \rangle$ in parameter space. A critical temperature arises whenever this trajectory crosses a critical surface.

Table 1. Parameter values for eight teleost embryos. To the left: L , volume to surface area ratio [m]; m , maximum consumption rate [$\text{kg} (\text{m}^{-3}\text{s}^{-1})$]; D , diffusion coefficient [$\text{m}^2 \text{s}^{-1}$]; C_∞ , free water oxygen concentration [kg m^{-3}]. The mass transfer coefficient $k_{\text{eff}} = 3.00 \cdot 10^{-5} \text{ m s}^{-1}$ for all eight embryos. To the right: P , dimensionless consumption rate; Q , dimensionless mass transfer coefficient. The dimensionless parameters S and T are defined in Section 5.

| | $\frac{L}{\times 10^{-5}}$ | $\frac{m}{\times 10^{-4}}$ | $\frac{D}{\times 10^{-10}}$ | $\frac{C_\infty}{\times 10^{-3}}$ | P | Q | S | T |
|--------------------------------------|----------------------------|----------------------------|-----------------------------|-----------------------------------|------|------|------|------|
| African catfish | | | | | | | | |
| <i>Clarias gariepinus</i> | 8.50 | 3.80 | 7.41 | 8.19 | 0.45 | 3.44 | 5.12 | 0.67 |
| Common carp | | | | | | | | |
| <i>Cyprinus carpio</i> | 6.20 | 11.0 | 6.55 | 9.00 | 0.72 | 2.84 | 3.35 | 0.85 |
| Herring | | | | | | | | |
| <i>Clupea harengus</i> | 12.0 | 0.430 | 5.47 | 10.5 | 0.11 | 6.58 | 20.0 | 0.33 |
| Largemouth bass | | | | | | | | |
| <i>Micropterus salmoides</i> | 10.0 | 3.70 | 6.55 | 9.00 | 0.63 | 4.58 | 5.78 | 0.79 |
| Plaice | | | | | | | | |
| <i>Pleuronectes platessa</i> | 8.70 | 1.70 | 5.05 | 11.2 | 0.23 | 5.17 | 10.8 | 0.48 |
| Rabbitfish | | | | | | | | |
| <i>Siganus randalli</i> | 4.80 | 2.80 | 7.96 | 7.76 | 0.10 | 1.81 | 5.60 | 0.32 |
| Winter flounder | | | | | | | | |
| <i>Pseudopleuronectes americanus</i> | 5.60 | 4.80 | 4.59 | 12.2 | 0.03 | 3.66 | 22.3 | 0.38 |
| Zebrafish | | | | | | | | |
| <i>Danio rerio</i> | 4.60 | 4.10 | 7.41 | 8.19 | 0.14 | 1.86 | 4.93 | 0.38 |

One more example: because we are particularly interested in how the size of an organism affects its equilibrium state, it is worthwhile noting that if we multiply the size of G by κ , P changes into $P\kappa^2$, Q into $Q\kappa$ (and, to be complete, τ into τ/κ). Therefore, points in parameter space representing different sizes of the organism, all other circumstances unchanged, are to be found on a simple parabola parallel with the PQ -plane. A critical size for an organism corresponds with a point of intersection of this parabola and S_{reg} or S_{conf} .

Another measurable quantity predicted by our model is the mean (oxygen) consumption rate γ , that is the consumption rate per unit of volume:

$$\gamma = \frac{1}{V} \int_G F(u(\vec{x})) d\omega = \frac{D}{V} \int_{\partial G} \frac{\partial}{\partial \vec{n}} u(\vec{x}) d\sigma. \quad (2.15)$$

With dimensionless volume $V' = \int_{G'} 1 d\omega'$ and dimensionless surface area $A' = \int_{\partial G'} 1 d\sigma'$ (remember: $V'/A' = 1$) the corresponding dimensionless mean consumption rate Γ is given by:

$$\Gamma = \frac{1}{V'} \int_{G'} \Phi(v(\vec{\xi})) d\omega' = \frac{1}{A'} \int_{\partial G'} \frac{\partial}{\partial \vec{n}'} v(\vec{\xi}) d\sigma', \quad (2.16)$$

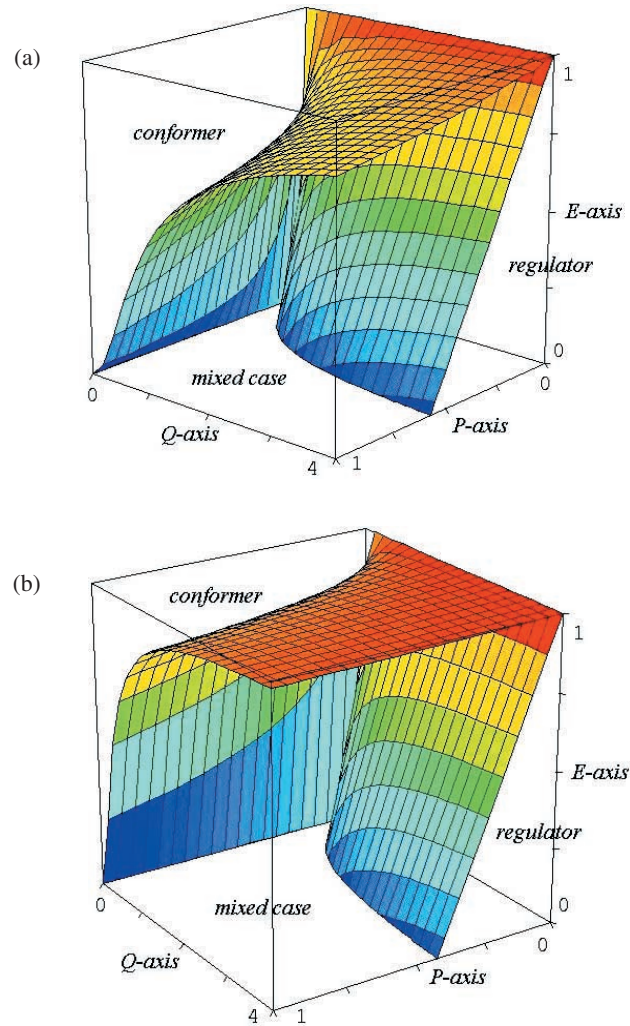


Figure 2. For (a) the sphere, and (b) the cube, and for $K = 1$: the critical surfaces S_{reg} and S_{conf} divide the reduced parameter space $\langle P, Q, E, 1 \rangle$ into three parts: the regulator domain (oxygen deficiency nowhere in the organism), the mixed domain (oxygen deficiency somewhere in the organism), the conformer domain (oxygen deficiency everywhere in the organism). For differently shaped organisms the picture is essentially the same.

which means that Γ also equals the mean dimensionless surface flux. The relation between γ and Γ is given by the equality: $\gamma t = \Gamma \tau C_{\infty}$.

Of course Γ is a function of the model parameters P, Q, E, K , but Γ also depends on the type G' of the organism under consideration. For a pure regulator we have of course $\Gamma = P$; for other cases we can use Γ to determine what shape of an organism is a more favourable one (that is, admits a higher value for Γ , or, allows a better overall respiration), given all other circumstances are the same [see Fig. 3(b)].

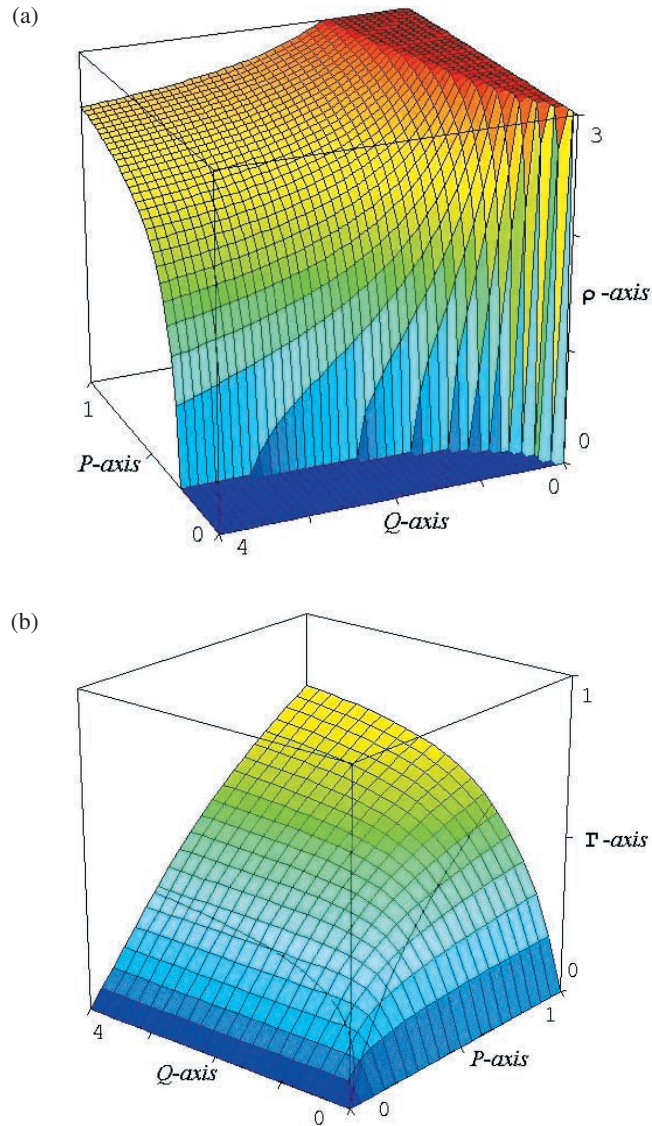


Figure 3. For the sphere and for $K = 1$, $E = \frac{1}{2}$. (a) The radius ρ of the region with conformer behaviour as a function of the dimensionless maximum consumption rate P and the dimensionless mass transfer coefficient Q . For a pure regulator $\rho = 0$; for a pure conformer $\rho = 3$. (b) The dimensionless mean consumption rate Γ as a function of the dimensionless maximum consumption rate P and the dimensionless mass transfer coefficient Q . The two extra curves on the surface separate pure regulator behaviour from mixed case behaviour and mixed case behaviour from pure conformer behaviour.

3. ONE-DIMENSIONAL CASES

In this section we demonstrate the principles set out in the previous section for three simple cases: the infinite sheet, the infinite cylinder and the sphere. At first

glance an organism in the form of an infinite sheet or an infinite cylinder seems strange. But firstly, we need only a perpendicular cross-section of such a sheet or cylinder; the resulting extra surface we render ineffective by taking there a homogeneous boundary condition of the second kind (a no-flow boundary condition). And secondly, later on we will see that the case of a (thin) finite sheet or a (long) finite cylinder may be readily approximated by the corresponding infinite case.

The common feature of these three cases is their inherent symmetry, which allows for the use of only one place variable: all three cases are effectively 1D. Consequently, for all these cases (2.12) and (2.13) reduce to simple ordinary differential equations with matching boundary conditions. The case of the infinite sheet we will discuss in some detail. For the infinite cylinder and the sphere we will only give the final results.

3.1. The infinite sheet. The volume to surface area ratio for (any perpendicular cross-section of) a plane infinite sheet with diameter $2R$ equals R . Therefore the (dimensionless) diameter of the ‘standard’ infinite sheet equals 2. Hence we may reduce (2.12) and (2.13) to the following boundary value problem on $[0, 1]$:

$$\text{ODE: } \frac{\partial^2}{\partial \xi^2} v(\xi) - \Phi(v(\xi)) = 0, \quad \text{for } 0 < \xi < 1; \quad (3.1)$$

$$\text{BC}_1: \frac{\partial}{\partial \xi} v(0) = 0, \quad \text{BC}_2: \frac{\partial}{\partial \xi} v(1) + \frac{Q}{K} v(1) = Q. \quad (3.2)$$

This boundary value problem is easily solved for the (pure) regulator or (pure) conformer case. The regulator case occurs if (and only if) $v(0) \geq E$. Now $\Phi(v) = P$ and it follows that

$$v(\xi) = \frac{P}{2} \xi^2 + K - \frac{KP}{Q} - \frac{P}{2}. \quad (3.3)$$

The conformer case occurs if (and only if) $v(1) \leq E$. Now $\Phi(v) = Pv/E$ and it follows that

$$v(\xi) = \frac{KQ \cosh(\xi \sqrt{P/E})}{K \sqrt{P/E} \sinh(\sqrt{P/E}) + Q \cosh(\sqrt{P/E})}. \quad (3.4)$$

Expressions for the critical surfaces follow already from equations (3.3) and (3.4):

$$S_{\text{reg}} : (K - E)Q = KP + PQ/2, \quad (3.5)$$

$$S_{\text{conf}} : (K - E)Q = KE \sqrt{P/E} \tanh(\sqrt{P/E}). \quad (3.6)$$

For a mixed case there will be, for some ρ between 0 and 1, conformer behaviour on $[0, \rho]$ and regulator behaviour on $[\rho, 1]$. By means of the (continuity) conditions

$$\lim_{\xi \uparrow \rho} v(\xi) = E, \quad \lim_{\xi \downarrow \rho} v(\xi) = E, \quad \text{and} \quad \lim_{\xi \uparrow \rho} \frac{\partial}{\partial \xi} v(\xi) = \lim_{\xi \downarrow \rho} \frac{\partial}{\partial \xi} v(\xi) \quad (3.7)$$

we find for $0 \leq \xi \leq \rho$:

$$v(\xi) = E \frac{\cosh(\xi\sqrt{P/E})}{\cosh(\rho\sqrt{P/E})}, \quad (3.8)$$

and for $\rho \leq \xi \leq 1$:

$$v(\xi) = \frac{P}{2} \xi^2 + \frac{2(K-E)Q - 2KP - PQ(1-\rho^2)}{2K + 2Q(1-\rho)} \left(\xi - 1 - \frac{K}{Q} \right) + K - \frac{KP}{Q} - \frac{P}{2}, \quad (3.9)$$

with ρ the (unique) root between 0 and 1 of the following transcendental equation:

$$E\sqrt{P/E} \tanh(\rho\sqrt{P/E}) = \frac{2(K-E)Q - 2KP(1-\rho) - PQ(1-\rho)^2}{2K + 2Q(1-\rho)}. \quad (3.10)$$

Obviously we should give ρ the value 0 for a (pure) regulator, while for a (pure) conformer ρ should get the value 1. Then, as expected, equation (3.10) reduces for $\rho = 0$ to (3.5) and for $\rho = 1$ to (3.6).

The dimensionless mean consumption rate Γ follows from (2.16). For this simple 1D case it holds that

$$\Gamma = \frac{\partial}{\partial \xi} v(1). \quad (3.11)$$

Hence from equations (3.3), (3.4) and (3.9) we infer (respectively):

$$\Gamma = P, \quad \text{for a regulator;} \quad (3.12)$$

$$\Gamma = \frac{KQ}{K + Q\sqrt{E/P} \coth(\sqrt{P/E})}, \quad \text{for a conformer;} \quad (3.13)$$

$$\Gamma = \frac{2(K-E)Q + PQ(1-\rho)^2}{2K + 2Q(1-\rho)}, \quad \text{for a mixed case.} \quad (3.14)$$

The result for a regulator is, of course, not a surprise: it follows also from first principles or, for that matter, from (2.16). Note that equation (3.14) on S_{reg} reduces to (3.12) and on S_{conf} to (3.13).

3.2. The infinite cylinder and the sphere. The case of the infinite cylinder and the sphere can be treated in exactly the same way. For that reason we mention in this subsection only the relevant model equations and their most important consequences.

First we discuss the case of the infinite cylinder. The (dimensionless) radius of the ‘standard’ infinite cylinder equals 2; therefore we have to solve the following boundary value problem on $[0, 2]$:

$$\text{ODE: } \frac{1}{\xi} \frac{\partial}{\partial \xi} \left[\xi \frac{\partial}{\partial \xi} v(\xi) \right] - \Phi(v(\xi)) = 0, \quad \text{for } 0 < \xi < 2; \quad (3.15)$$

$$\text{BC}_1: \lim_{\xi \rightarrow 0} \xi \frac{\partial}{\partial \xi} v(\xi) = 0, \quad \text{BC}_2: \frac{\partial}{\partial \xi} v(2) + \frac{Q}{K} v(2) = Q. \quad (3.16)$$

The expressions for the critical surfaces are:

$$S_{\text{reg}} : (K - E)Q = KP + PQ, \quad (3.17)$$

$$S_{\text{conf}} : (K - E)Q = KE\sqrt{P/E} I_1(2\sqrt{P/E})/I_0(2\sqrt{P/E}), \quad (3.18)$$

where I_0 and I_1 are modified Bessel functions (Abramowitz and Stegun, 1965). The transcendental equation for the radius ρ of the region with conformer behaviour reads:

$$\begin{aligned} E\sqrt{P/E} \frac{I_1(\rho\sqrt{P/E})}{I_0(\rho\sqrt{P/E})} \\ = \frac{2(K - E)Q - 2(PQ + KP)(1 - \rho^2/4) - PQ\rho^2 \ln(\rho/2)}{K\rho - 2Q\rho \ln(\rho/2)}. \end{aligned} \quad (3.19)$$

This time ρ should have the value 2 for a (pure) conformer. As expected, equation (3.19) reduces for $\rho = 0$ to (3.17) and for $\rho = 2$ to (3.18).

The (dimensionless) mean consumption rate Γ for this case is given by:

$$\Gamma = P, \quad \text{for a regulator;} \quad (3.20)$$

$$\Gamma = \frac{KQ\sqrt{P/E} I_1(2\sqrt{P/E})}{K\sqrt{P/E} I_1(2\sqrt{P/E}) + Q I_0(2\sqrt{P/E})}, \quad \text{for a conformer;} \quad (3.21)$$

$$\Gamma = \frac{(K - E)Q - PQ(1 - \rho^2/4) - 2PQ \ln(\rho/2)}{K - 2Q \ln(\rho/2)}, \quad \text{for a mixed case.} \quad (3.22)$$

Note again that equation (3.22) reduces on S_{reg} to (3.20) and on S_{conf} to (3.21).

Next we discuss the case of a spherical organism. The (dimensionless) radius of the 'standard' sphere equals 3; therefore we have to solve the following boundary value problem on $[0, 3]$:

$$\text{ODE: } \frac{1}{\xi^2} \frac{\partial}{\partial \xi} \left[\xi^2 \frac{\partial}{\partial \xi} v(\xi) \right] - \Phi(v(\xi)) = 0, \quad \text{for } 0 < \xi < 3; \quad (3.23)$$

$$\text{BC}_1: \lim_{\xi \rightarrow 0} \xi^2 \frac{\partial}{\partial \xi} v(\xi) = 0, \quad \text{BC}_2: \frac{\partial}{\partial \xi} v(3) + \frac{Q}{K} v(3) = Q. \quad (3.24)$$

The expressions for the critical surfaces [see Fig. 2(a)] are:

$$S_{\text{reg}} : (K - E)Q = KP + 3PQ/2, \quad (3.25)$$

$$S_{\text{conf}} : (K - E)Q = KE(\sqrt{P/E} \coth(3\sqrt{P/E}) - 1/3). \quad (3.26)$$

Comparison of the values for P and Q in Table 1 with Fig. 2 shows, as follows from (3.25), that for the chosen values of E (≈ 0.01) and K ($= 1$), zebrafish,

rabbitfish, winter flounder, plaice and herring are clearly in the regulator area (in both the sphere and the cube model). Common carp and largemouth bass are in the mixed case area. African catfish enters the mixed case area when going from the sphere to the cube model.

The transcendental equation for the radius ρ of the region with conformer behaviour is given by:

$$\begin{aligned} & E(\rho\sqrt{P/E} \coth(\rho\sqrt{P/E}) - 1) \\ &= \frac{9(K-E)Q - 9KP(1 - \rho^3/27) - 9PQ(1 - \rho/3)^2(\rho + 3/2)}{K\rho + 3Q(3 - \rho)}. \end{aligned} \quad (3.27)$$

For this case ρ should have the value 3 for a (pure) conformer. Again, equation (3.27) reduces for $\rho = 0$ to (3.25) and for $\rho = 3$ to (3.26). Finally, the (dimensionless) mean consumption rate Γ is given by:

$$\Gamma = P, \quad \text{for a regulator;} \quad (3.28)$$

$$\Gamma = \frac{KQ(\sqrt{P/E} \coth(3\sqrt{P/E}) - 1/3)}{K(\sqrt{P/E} \coth(3\sqrt{P/E}) - 1/3) + Q}, \quad \text{for a conformer;} \quad (3.29)$$

$$\Gamma = \frac{(K-E)Q\rho + 9PQ(1 - \rho/3)^2(1 + \rho/6)}{K\rho + 9Q(1 - \rho/3)}, \quad \text{for a mixed case.} \quad (3.30)$$

See Fig. 3. Again, equation (3.30) reduces to (3.28) on S_{reg} and reduces to (3.29) on S_{conf} .

3.3. Limit cases and critical sizes. Several interesting special cases are neatly incorporated in our formalism. We discuss these cases mainly for an infinite sheet. It is easily verified that analogous results can be achieved for the infinite cylinder and for the sphere, or even for arbitrarily shaped organisms.

(1) In the literature (Byatt-Smith *et al.*, 1991), the term conformer is used if the oxygen consumption rate F the organism exhibits is modelled by a linear function: $F(u) = au$ (in dimensionless form: $\Phi(v) = pv$), while the term regulator is used if F is modelled by a constant function: $F(u) = m$ (in dimensionless form: $\Phi(v) = P$).

The first of these two special cases is represented within our model by the condition $E \geq K$. Because K obviously is an upper limit for the dimensionless oxygen concentration v inside the organism, the condition $E \geq K$ compels conformer behaviour everywhere in the organism, independent of all other parameter values. We could introduce for this case the new (dimensionless) variable $p = P/E$, thereby removing one parameter from our model [note the occurrence of the term P/E in (3.4) and (3.13)]. The model equations for this case are linear: now even the time-dependent equations are easily solvable.

The second special case is represented within our model by the condition $E = 0$. It should be noted that this case still leaves open the possibility of conformer behaviour somewhere in the organism. Conformer behaviour in this case just means that the oxygen concentration v in part of the organism is equal to zero, see equation (3.8). The transition from pure regulator behaviour to partial conformer behaviour is still given by (3.5). Even pure conformer behaviour is possible for this case: this also happens if $Q = 0$, as follows from (3.6). Because $Q = 0$ stands for a homogeneous boundary condition of the second kind (a no-flow boundary condition), this is as expected. For $E = 0$ the transcendental equation (3.10) for the ‘radius’ ρ of the region with conformer behaviour reduces to a simple quadratic equation. So for this special case it follows from (3.10) and (3.14) that the dimensionless consumption rate $\Gamma = P(1 - \rho)$, which for this simple case also follows from first principles.

(2) That leaves the case $0 < E < K$. Now all three behavioural patterns are possible: the organism may be a pure regulator, or may be in a mixed state, or may be a pure conformer. The critical surfaces S_{reg} and S_{conf} separate these three possibilities in parameter space, see Fig. 2.

As already said before, the limiting case $Q = \infty$ ($k_{\text{eff}} = \infty$) is tied in with so-called running water conditions, or well-stirred water conditions (Carslaw and Jaeger, 1959; Kranenbarg *et al.*, 2001). For this special case the second boundary condition (3.2b) changes into a simple boundary condition of the first kind, BC_2 : $v(1) = K$. The expressions for the critical surfaces, given by (3.5) and (3.6), simplify to S_{reg} : $K - E = P/2$ and S_{conf} : $K - E = 0$; therefore pure conformer behaviour is impossible for this limit case (unless $E \geq K$).

(3) Special attention is often devoted to that size of an (slowly growing) organism, for which it first encounters, somewhere in its interior, oxygen deficiency. Such a size is called a critical size. Because oxygen is needed to perform essential biological processes, natural selection will favour organisms that prevent oxygen deficiency in their interior. These organisms can either stay of subcritical size or develop an additional oxygen transport system (e.g., a circulatory system) by the time they reach their critical size. Within our model oxygen deficiency starts when the representation $\langle P, Q, E, K \rangle$ of this organism in parameter space passes the critical surface S_{reg} . Therefore, as follows from equations (3.5), (3.17) and (3.25), for such a critical point it holds that

$$(K - E)Q = KP + nPQ/2, \quad (3.31)$$

where it is understood that n takes the value 1 for an infinite sheet, 2 for an infinite cylinder and 3 for a sphere. We divide equation (3.31) by Q , rewrite the result with the help of (2.11) in terms of the original model parameters, to find, after some rearrangements:

$$\frac{n}{2}L^2 + \frac{KD}{k_{\text{eff}}}L - \frac{D}{m}(KC_{\infty} - C_0) = 0. \quad (3.32)$$

Hence for the critical value of the volume to surface area ratio we obtain:

$$L_{\text{crit}} = -\frac{KD}{nk_{\text{eff}}} + \sqrt{\frac{K^2 D^2}{n^2 k_{\text{eff}}^2} + \frac{2D}{nm} (KC_{\infty} - C_0)}. \quad (3.33)$$

Note that L_{crit} represents the maximum volume of respiring tissue that can be fully supplied with oxygen per unit surface area. With R_{crit} the critical radius (half the diameter) of the object under consideration, it follows from the relation $L = V/A = R/n$ that

$$R_{\text{crit}} = -\frac{KD}{k_{\text{eff}}} + \frac{KD}{k_{\text{eff}}} \sqrt{1 + 2n \frac{k_{\text{eff}}^2}{mKD} \left(C_{\infty} - \frac{C_0}{K} \right)}. \quad (3.34)$$

The special case $C_0 = 0$, $K = 1$ and $k_{\text{eff}} = \infty$ yields

$$R_{\text{crit}} = \sqrt{2n \frac{DC_{\infty}}{m}}, \quad (3.35)$$

a well-known result [e.g., Graham (1988)]. Note that it is possible to determine in exactly the same way critical values for other model parameters.

(4) One more interesting limit case arises when we take the thickness δ of the static fluid film that surrounds the organism to infinity. This situation can be simulated in the laboratory by placing one small organism at the centre of a large water-filled tank. For an infinite sheet and an infinite cylinder taking δ to infinity means that k_{eff} goes to zero. The reason for this is the nonexistence of a stationary solution for the diffusion problem outside the organism for these two shapes. Though for a sphere-like organism, say with radius R , such an external stationary solution does exist: $u_{\text{ex}}(x) = C_{\infty} + (u(R)/K - C_{\infty})R/x$, with $x > R$ the distance from the centre of the sphere. It follows that k_{eff} takes the value $D_w/R = D_w/(3L)$, with D_w again the diffusion coefficient of oxygen in water. Substituting this value for k_{eff} in (3.32) we obtain:

$$\left(\frac{3}{2} + \frac{3KD}{D_w} \right) L^2 - \frac{D}{m} (KC_{\infty} - C_0) = 0. \quad (3.36)$$

So the critical value of the volume to surface area ratio for this case is:

$$L_{\text{crit}} = \sqrt{\frac{2D_w D (KC_{\infty} - C_0)}{3m(D_w + 2KD)}}. \quad (3.37)$$

The special case $C_0 = 0$ and $K = 1$ yields:

$$L_{\text{crit}} = \sqrt{\frac{2D_w DC_{\infty}}{3m(D_w + 2D)}}, \quad (3.38)$$

also a well-known result [e.g., Lee and Strathmann (1998)].

(5) Finally we discuss the question: what happens at the critical surface S_{conf} ? Will a growing organism, beyond its critical size, eventually change into a pure conformer, or will it always remain in a mixed state? For the infinite sheet this question is answered by means of equation (3.6). Rewriting this equation in terms of the original model parameters, see (2.11), we obtain after some rearrangements:

$$k_{\text{eff}} \left(C_{\infty} - \frac{C_0}{K} \right) = \sqrt{mDC_0} \tanh \left(L \sqrt{\frac{m}{DC_0}} \right). \quad (3.39)$$

Therefore, if it holds that

$$k_{\text{eff}} \left(C_{\infty} - \frac{C_0}{K} \right) \geq \sqrt{mDC_0}, \quad (3.40)$$

a growing organism of this shape will always retain a region with regulator behaviour, which is the case for all eight teleost embryos in Table 1. A simple inspection of the right-hand side of equations (3.18) and (3.26) shows that the same condition applies for an infinite cylinder and for a sphere.

We will show that this condition also holds for an organism of arbitrary shape. With that goal in mind we put a given point on a smooth part of the surface ∂G of the organism under a magnifying-glass: in this way we interpret the organism in the neighbourhood of this point as a (left) half-space. Then, assuming that the organism is a pure conformer, the following initial value problem describes the tendency of the system in the neighbourhood of this point, see equations (2.8) and (2.9):

$$\text{PDE: } \frac{\partial}{\partial \tau} v(\xi, \tau) = \frac{\partial^2}{\partial \xi^2} v(\xi, \tau) - \frac{P}{E} v(\xi, \tau), \quad \text{for } \xi < 0 \text{ and } \tau > 0; \quad (3.41)$$

$$\text{BC: } \frac{\partial}{\partial \xi} v(0, \tau) + \frac{Q}{K} v(0, \tau) = Q, \quad \text{IC: } v(\xi, 0) = v_0. \quad (3.42)$$

Next we apply the Laplace transformation: $v(\xi, \tau) \rightarrow V(\xi, s)$. A straightforward calculation yields:

$$V(\xi, s) = \frac{v_0}{s + P/E} + \left(\frac{Q}{s} - \frac{v_0 Q/K}{s + P/E} \right) \frac{\exp(\xi \sqrt{s + P/E})}{Q/K + \sqrt{s + P/E}}. \quad (3.43)$$

It follows:

$$\lim_{\tau \rightarrow \infty} v(0, \tau) = \lim_{s \downarrow 0} s V(0, s) = \frac{Q}{Q/K + \sqrt{P/E}}. \quad (3.44)$$

Thus a condition for regulator behaviour in the neighbourhood of this point is:

$$\frac{Q}{Q/K + \sqrt{P/E}} \geq E. \quad (3.45)$$

If we rewrite this result with the help of (2.11) in terms of the original model parameters, we retrieve equation (3.40).

4. HIGHER-DIMENSIONAL CASES

In Section 3 we provided a complete analytical solution of the nonlinear boundary value problem stated in equations (2.12) and (2.13) for three 1D cases. Such a general solution is not feasible for higher-dimensional cases. The difficulty here is the description of the surface inside the organism that separates the region with regulator behaviour from the region with conformer behaviour. But if we restrict ourselves to the pure regulator case or to the pure conformer case the problem simplifies to a linear boundary value problem and a solution by the method of eigenfunction expansion becomes possible. This method enables us to obtain useful expressions for the critical surfaces S_{reg} and S_{conf} for higher-dimensional cases.

4.1. A formal solution. We consider the following eigenvalue problem, which will prove to be central to our purpose:

$$\text{PDE: } \Delta_{\vec{\xi}} X(\vec{\xi}) + \lambda X(\vec{\xi}) = 0, \quad \text{for } \vec{\xi} \in G'; \quad (4.1)$$

$$\text{BC: } \frac{\partial}{\partial \vec{n}'} X(\vec{\xi}) + \frac{Q}{K} X(\vec{\xi}) = 0, \quad \text{for } \vec{\xi} \in \partial G'. \quad (4.2)$$

Such an eigenvalue problem admits an infinite number of (positive) eigenvalues λ_n with corresponding eigenfunctions $X_n(\vec{\xi})$ ($n = 1, 2, 3, \dots$) [cf. Churchill (1955)]. If we expand the constant function $g(\vec{\xi}) = 1$ on G' with respect to this (orthogonal) set of eigenfunctions, the result is:

$$\begin{aligned} 1 &= \sum_{n=1}^{\infty} \gamma_n X_n(\vec{\xi}), \quad \text{with } \gamma_n = (g, X_n) / (X_n, X_n) \\ &= \int_{G'} X_n(\vec{\xi}) d\omega' / \int_{G'} X_n(\vec{\xi})^2 d\omega'. \end{aligned} \quad (4.3)$$

As we will shortly see, both special cases mentioned are solvable in terms of the eigenfunctions $X_n(\vec{\xi})$, the eigenvalues λ_n , and the Fourier coefficients γ_n .

For a *pure regulator* it holds that $v(\vec{\xi}) \geq E$ for all $\vec{\xi} \in G'$. This means that $\Phi(v) = P$, as follows from (2.10). Then equations (2.12) and (2.13) reduce to:

$$\text{PDE: } \Delta_{\vec{\xi}} v(\vec{\xi}) = P, \quad \text{for } \vec{\xi} \in G'; \quad (4.4)$$

$$\text{BC: } \frac{\partial}{\partial \vec{n}'} v(\vec{\xi}) + \frac{Q}{K} v(\vec{\xi}) = Q, \quad \text{for } \vec{\xi} \in \partial G'. \quad (4.5)$$

The formal solution of this problem is:

$$v_{\text{reg}}(\vec{\xi}) = K - P \sum_{n=1}^{\infty} \frac{\gamma_n}{\lambda_n} X_n(\vec{\xi}), \quad (4.6)$$

as follows easily by inspection. The critical surface S_{reg} is given by $\min_{\vec{\xi} \in G'} [v_{\text{reg}}(\vec{\xi})] = E$, see (2.14). This yields the following equation for the critical surface:

$$S_{\text{reg}} : \quad K - E = P \max_{\vec{\xi} \in G'} \left(\sum_{n=1}^{\infty} \frac{\gamma_n}{\lambda_n} X_n(\vec{\xi}) \right). \quad (4.7)$$

For a *pure conformer* it holds that $v(\vec{\xi}) \leq E$ for all $\vec{\xi} \in G'$. This means that $\Phi(v) = Pv/E$, see, again, (2.10). So this time equations (2.12) and (2.13) reduce to:

$$\text{PDE: } \Delta_{\vec{\xi}} v(\vec{\xi}) - \frac{P}{E} v(\vec{\xi}) = 0, \quad \text{for } \vec{\xi} \in G'; \quad (4.8)$$

$$\text{BC: } \frac{\partial}{\partial \vec{n}'} v(\vec{\xi}) + \frac{Q}{K} v(\vec{\xi}) = Q, \quad \text{for } \vec{\xi} \in \partial G'. \quad (4.9)$$

The formal solution of this problem is:

$$v_{\text{conf}}(\vec{\xi}) = K - K(P/E) \sum_{n=1}^{\infty} \frac{\gamma_n}{P/E + \lambda_n} X_n(\vec{\xi}), \quad (4.10)$$

as follows again by inspection. The second critical surface S_{conf} is given by $\max_{\vec{\xi} \in G'} [v_{\text{conf}}(\vec{\xi})] = E$, see, again, (2.14). This yields the following equation for the critical surface:

$$S_{\text{conf}} : \quad K - E = K(P/E) \min_{\vec{\xi} \in G'} \left(\sum_{n=1}^{\infty} \frac{\gamma_n}{P/E + \lambda_n} X_n(\vec{\xi}) \right). \quad (4.11)$$

For a pure regulator the *dimensionless oxygen consumption rate* $\Gamma = P$, as follows from first principles or, for that matter, from the first equality in equation (2.16). For a pure conformer it follows from (4.10) and the second equality in equation (2.16) that

$$\Gamma = -K(P/E)/A' \sum_{n=1}^{\infty} \frac{\gamma_n}{P/E + \lambda_n} \int_{\partial G'} \frac{\partial}{\partial \vec{n}'} X_n(\vec{\xi}) d\sigma'. \quad (4.12)$$

An application of Green's identity on the surface integral in the right-hand side of equation (4.12) yields, together with (4.1):

$$\Gamma = K(P/E)/A' \sum_{n=1}^{\infty} \frac{\gamma_n \lambda_n}{P/E + \lambda_n} \int_{G'} X_n(\vec{\xi}) d\omega'. \quad (4.13)$$

Parseval's relation for the constant function $g(\vec{\xi}) = 1$ on G' yields, together with (4.3):

$$V' = (g, g) = \sum_{n=1}^{\infty} (g, X_n)^2 / (X_n, X_n) = \sum_{n=1}^{\infty} \gamma_n \int_{G'} X_n(\vec{\xi}) d\omega'. \quad (4.14)$$

Next we define: $g_n = \frac{\gamma_n}{V'} \int_{G'} X_n(\vec{\xi}) d\omega'$, which means: $\sum_{n=1}^{\infty} g_n = 1$. (4.15)

In this way we obtain from (4.13) and (4.15), and with the equality $V' = A'$ in mind, the following concise expression for the dimensionless consumption rate Γ for a pure conformer:

$$\Gamma = K(P/E) \sum_{n=1}^{\infty} \frac{g_n \lambda_n}{P/E + \lambda_n}. \quad (4.16)$$

Note that the parameter combination Q/K plays a role in the determination of the eigenvalues λ_n and the weight factors g_n .

4.2. Three characteristic shapes. It should be noted that it is not always possible to find an analytical solution for the eigenvalue problem stated in (4.1) and (4.2). For exotic regions G' we have to use numerical methods, for instance, a Galerkin procedure (Fairweather, 1978). But for (from a mathematical point of view) reasonably shaped organisms an explicit solution is attainable [cf. Gielen (2000)]. The regions G' discussed in the following three examples, are determined by one or two shape-parameters. We use these parameters in Section 5 to distinguish and compare between elongated, compact and sheet-like organisms.

4.2.1. Infinite beam. First we discuss in some detail the case of a (rectangular) infinite beam with length $2R_1$ and breadth $2R_2$. We may take $R_1 \leq R_2$, which means that $\alpha = R_2/R_1 \geq 1$. Note that α defines the shape of the beam and that the 'dimensions' of the standard beam of this shape are $2(1 + 1/\alpha)$ and $2(1 + \alpha)$, respectively. With $G' = [-1 - 1/\alpha, 1 + 1/\alpha] \times [-1 - \alpha, 1 + \alpha]$ equations (2.12) and (2.13) constitute a two-dimensional boundary value problem.

Because of the inherent symmetry of the case under consideration, it is obvious that in the equilibrium situation there will be no oxygen transport through the planes $\xi_1 = 0$ and $\xi_2 = 0$. Therefore it is possible to restrict the problem to the region $[0, 1 + 1/\alpha] \times [0, 1 + \alpha]$ by taking no-flow boundary conditions on these planes. Then the eigenvalue problem stated in (4.1) and (4.2) may be written as:

$$\text{PDE: } \frac{\partial^2}{\partial \xi_1^2} X(\xi_1, \xi_2) + \frac{\partial^2}{\partial \xi_2^2} X(\xi_1, \xi_2) + \lambda X(\xi_1, \xi_2) = 0, \quad (4.17)$$

$$\begin{aligned} \text{BC}_1: \frac{\partial}{\partial \xi_1} X(0, \xi_2) = 0, \quad \text{BC}_2: \frac{\partial}{\partial \xi_1} X(1 + 1/\alpha, \xi_2) \\ + \frac{Q}{K} X(1 + 1/\alpha, \xi_2) = 0, \end{aligned} \quad (4.18)$$

$$\begin{aligned} \text{BC}_3: \frac{\partial}{\partial \xi_2} X(\xi_1, 0) = 0, \quad \text{BC}_4: \frac{\partial}{\partial \xi_2} X(\xi_1, 1 + \alpha) \\ + \frac{Q}{K} X(\xi_1, 1 + \alpha) = 0. \end{aligned} \quad (4.19)$$

Applying the well-known separation of variables technique: $X(\xi_1, \xi_2) = \tilde{X}_1(\xi_1) \tilde{X}_2(\xi_2)$, we obtain two (almost identical) so-called regular Sturm–Liouville problems:

$$\begin{cases} \tilde{X}_1''(\xi_1) + \lambda_1 \tilde{X}_1(\xi_1) = 0, & \text{for } 0 < \xi_1 < 1 + 1/\alpha, \\ \tilde{X}_1'(0) = 0, \\ \tilde{X}_1'(1 + 1/\alpha) + (Q/K) \tilde{X}_1(1 + 1/\alpha) = 0; \end{cases} \quad (4.20)$$

$$\begin{cases} \tilde{X}_2''(\xi_2) + \lambda_2 \tilde{X}_2(\xi_2) = 0, & \text{for } 0 < \xi_2 < 1 + \alpha, \\ \tilde{X}_2'(0) = 0, \\ \tilde{X}_2'(1 + \alpha) + (Q/K) \tilde{X}_2(1 + \alpha) = 0. \end{cases} \quad (4.21)$$

Because $Q/K > 0$ the eigenvalues $\lambda_{1,n}$ and $\lambda_{2,n}$ are positive: we write $\lambda_{1,n} = \mu_{1,n}^2$ with $\mu_{1,n} > 0$, and $\lambda_{2,n} = \mu_{2,n}^2$ with $\mu_{2,n} > 0$ ($n = 1, 2, 3, \dots$). A straightforward calculation yields the eigenfunctions:

$$\tilde{X}_{1,n}(\xi_1) = \cos(\mu_{1,n} \xi_1) \quad \text{and} \quad \tilde{X}_{2,n}(\xi_2) = \cos(\mu_{2,n} \xi_2), \quad (4.22)$$

where $\mu_{1,n}$ is the n th positive root of the first and where $\mu_{2,n}$ is the n th positive root of the second of the following two characteristic equations for μ :

$$\begin{aligned} -\mu K \sin(\mu(1 + 1/\alpha)) + Q \cos(\mu(1 + 1/\alpha)) = 0, \\ -\mu K \sin(\mu(1 + \alpha)) + Q \cos(\mu(1 + \alpha)) = 0. \end{aligned} \quad (4.23)$$

Hence the eigenfunctions $X_{i,j}(\xi_1, \xi_2)$ and corresponding eigenvalues $\lambda_{i,j}$ of the original problem are:

$$X_{i,j}(\xi_1, \xi_2) = \cos(\mu_{1,i} \xi_1) \cos(\mu_{2,j} \xi_2), \quad \text{with} \quad \lambda_{i,j} = \mu_{1,i}^2 + \mu_{2,j}^2. \quad (4.24)$$

Following the guideline set out in Section 4.1, we determine the Fourier coefficients $\gamma_{i,j}$ of the constant function $f(\xi_1, \xi_2) = 1$ with respect to this orthogonal set of eigenfunctions $X_{i,j}(\xi_1, \xi_2)$. It follows from equation (4.3) that

$$\gamma_{i,j} = \frac{\int_0^{1+1/\alpha} \tilde{X}_{1,i}(\xi_1) d\xi_1}{\int_0^{1+1/\alpha} \tilde{X}_{1,i}(\xi_1)^2 d\xi_1} \times \frac{\int_0^{1+\alpha} \tilde{X}_{2,j}(\xi_2) d\xi_2}{\int_0^{1+\alpha} \tilde{X}_{2,j}(\xi_2)^2 d\xi_2}, \quad (4.25)$$

which leads, with the shorthand $Q/K = q$, to

$$\gamma_{i,j} = \frac{2(-1)^{i+1}q\sqrt{q^2 + \mu_{1,i}^2}}{(1 + 1/\alpha)(\mu_{1,i}^3 + q^2\mu_{1,i}) + q\mu_{1,i}} \times \frac{2(-1)^{j+1}q\sqrt{q^2 + \mu_{2,j}^2}}{(1 + \alpha)(\mu_{2,j}^3 + q^2\mu_{2,j}) + q\mu_{2,j}}. \quad (4.26)$$

Once $\gamma_{i,j}$ is known, the dimensionless concentration $v_{\text{reg}}(\xi_1, \xi_2)$ follows from (4.6) and (4.24), and the dimensionless concentration $v_{\text{conf}}(\xi_1, \xi_2)$ follows from (4.10) and (4.24).

The next step, still following the path set out in Section 4.1, is the determination of the minimum value of $v_{\text{reg}}(\xi_1, \xi_2)$ and the maximum value of $v_{\text{conf}}(\xi_1, \xi_2)$ on G' . In general this is not an easy task; numerical methods may be needed, though for the highly symmetrical case we are dealing with here the problem is not that difficult. The minimum value of (any stationary) $v(\xi_1, \xi_2)$ on an infinite beam will always be found on the central axis of the beam and the maximum value will always be attained on the edges of the beam. In this way we infer from (4.7) and (4.11) for the critical surfaces the following equations:

$$S_{\text{reg}} : K - E = P \sum_{i,j=1}^{\infty} \frac{\gamma_{i,j}}{\mu_{1,i}^2 + \mu_{2,j}^2}, \quad (4.27)$$

$$S_{\text{conf}} : K - E = K(P/E) \sum_{i,j=1}^{\infty} \frac{\gamma_{i,j} \cos(\mu_{1,i}(1 + 1/\alpha)) \cos(\mu_{2,j}(1 + \alpha))}{P/E + \mu_{1,i}^2 + \mu_{2,j}^2}. \quad (4.28)$$

Note that the infinite sum in the right-hand side of (4.27) is a function of Q/K alone, while the infinite sum in the right-hand side of (4.28) is a function of Q/K and P/E .

4.2.2. Rectangular parallelepiped. Next we discuss the case of a (rectangular) parallelepiped with length $2R_1$, breadth $2R_2$ and height $2R_3$. We may take $R_1 \leq R_2 \leq R_3$, which means that $\alpha = R_2/R_1 \geq 1$ and $\beta = R_3/R_1 \geq \alpha$. The shape of the parallelepiped is fixed by α and β , and the ‘dimensions’ of the standard parallelepiped of this shape are $2(1 + 1/\alpha + 1/\beta)$, $2(1 + \alpha + \alpha/\beta)$ and $2(1 + \beta + \beta/\alpha)$, respectively. The symmetry argument already used for the case of an infinite beam yields, this time, a three-dimensional eigenvalue problem for an unknown function $X(\xi_1, \xi_2, \xi_3)$ on the region $[0, 1 + 1/\alpha + 1/\beta] \times [0, 1 + \alpha + \alpha/\beta] \times [0, 1 + \beta + \beta/\alpha]$.

The same reasoning as applied for the case of the infinite beam leads to the following eigenfunctions $X_{i,j,k}(\xi_1, \xi_2, \xi_3)$ and corresponding eigenvalues $\lambda_{i,j,k}$:

$$X_{i,j,k}(\xi_1, \xi_2, \xi_3) = \cos(\mu_{1,i}\xi_1) \cos(\mu_{2,j}\xi_2) \cos(\mu_{3,k}\xi_3),$$

with $\lambda_{i,j,k} = \mu_{1,i}^2 + \mu_{2,j}^2 + \mu_{3,k}^2, \quad (4.29)$

where $\mu_{1,n}$ is the n th positive root of the first, $\mu_{2,n}$ is the n th positive root of the second and $\mu_{3,n}$ is the n th positive root of the third of the following three characteristic equations for μ ($n = 1, 2, 3, \dots$):

$$\begin{aligned} -\mu K \sin(\mu(1 + 1/\alpha + 1/\beta)) + Q \cos(\mu(1 + 1/\alpha + 1/\beta)) &= 0, \\ -\mu K \sin(\mu(1 + \alpha + \alpha/\beta)) + Q \cos(\mu(1 + \alpha + \alpha/\beta)) &= 0, \quad (4.30) \\ -\mu K \sin(\mu(1 + \beta + \beta/\alpha)) + Q \cos(\mu(1 + \beta + \beta/\alpha)) &= 0. \end{aligned}$$

The Fourier coefficients $\gamma_{i,j,k}$ of the constant function $f(\xi_1, \xi_2, \xi_3) = 1$ with respect to this new orthogonal set of eigenfunctions are:

$$\begin{aligned} \gamma_{i,j,k} &= \frac{2(-1)^{i+1} q \sqrt{q^2 + \mu_{1,i}^2}}{(1 + 1/\alpha + 1/\beta)(\mu_{1,i}^3 + q^2 \mu_{1,i}) + q \mu_{1,i}} \\ &\quad \times \frac{2(-1)^{j+1} q \sqrt{q^2 + \mu_{2,j}^2}}{(1 + \alpha + \alpha/\beta)(\mu_{2,j}^3 + q^2 \mu_{2,j}) + q \mu_{2,j}} \\ &\quad \times \frac{2(-1)^{k+1} q \sqrt{q^2 + \mu_{3,k}^2}}{(1 + \beta + \beta/\alpha)(\mu_{3,k}^3 + q^2 \mu_{3,k}) + q \mu_{3,k}}, \quad (4.31) \end{aligned}$$

where, again, the shorthand $q = Q/K$ is used.

The minimum value of (any stationary) $v(\xi_1, \xi_2, \xi_3)$ on a rectangular parallelepiped will always be found in the centre and the maximum value will always be attained on the vertices. With these facts in mind we infer from (4.7) and (4.11) the following equations for the critical surfaces [see Fig. 2(b)]:

$$S_{\text{reg}} : \quad K - E = P \sum_{i,j,k=1}^{\infty} \frac{\gamma_{i,j,k}}{\mu_{1,i}^2 + \mu_{2,j}^2 + \mu_{3,k}^2}, \quad (4.32)$$

$$S_{\text{conf}} : \quad K - E = K(P/E) \quad (4.33)$$

$$\times \sum_{i,j,k=1}^{\infty} \frac{\gamma_{i,j,k} \cos(\mu_{1,i}(1 + 1/\alpha + 1/\beta)) \cos(\mu_{2,j}(1 + \alpha + \alpha/\beta)) \cos(\mu_{3,k}(1 + \beta + \beta/\alpha))}{P/E + \mu_{1,i}^2 + \mu_{2,j}^2 + \mu_{3,k}^2}.$$

If (for instance) we let β tend to infinity, then equations (4.30ab) transform into (4.23ab); hence the roots of (4.30ab) change into the roots of (4.23ab). And for the roots $\mu_{3,n}$ of equation (4.30c) it holds that $\mu_{3,n} \rightarrow 0$, but $\mu_{3,n}(1 + \beta + \beta/\alpha) \rightarrow (2n - 1)\pi/2$. Thus $\gamma_{i,j,k}$ changes into $\gamma_{i,j} (4/\pi)(-1)^{k+1}/(2k - 1)$, with $\gamma_{i,j}$ given by (4.26). By means of the well-known equality $\sum_{k=1}^{\infty} (-1)^{k+1}/(2k - 1) = \pi/4$ it follows that equation (4.32) transforms into (4.27). So we see that in this respect an elongated parallelepiped resembles an infinite beam. The same result can be obtained for equations (4.33) and (4.28), using a slightly more involved argument.

4.2.3. *Finite cylinder.* Finally we discuss the case of a finite cylinder with diameter $2R_1$ and length $2R_2$. The shape of the cylinder is again fixed by $\alpha = R_2/R_1$, this time with $0 < \alpha < \infty$, and the ‘dimensions’ of the standard finite cylinder of this shape are $2(2 + 1/\alpha)$ and $2(1 + 2\alpha)$, respectively. Symmetry arguments yield, in accordance with (4.1) and (4.2), a two-dimensional eigenvalue problem for an unknown function $X(\xi_1, \xi_2)$ on the region $[0, 2 + 1/\alpha] \times [0, 1 + 2\alpha]$:

$$\text{PDE: } \frac{1}{\xi_1} \frac{\partial}{\partial \xi_1} \left[\xi_1 \frac{\partial}{\partial \xi_1} X(\xi_1, \xi_2) \right] + \frac{\partial^2}{\partial \xi_2^2} X(\xi_1, \xi_2) + \lambda X(\xi_1, \xi_2) = 0, \quad (4.34)$$

$$\begin{aligned} \text{BC}_1: \lim_{\xi_1 \rightarrow 0} \xi_1 \frac{\partial}{\partial \xi_1} X(\xi_1, \xi_2) = 0, \quad \text{BC}_2: \frac{\partial}{\partial \xi_1} X(2 + 1/\alpha, \xi_2) \\ + \frac{Q}{K} X(2 + 1/\alpha, \xi_2) = 0, \end{aligned} \quad (4.35)$$

$$\begin{aligned} \text{BC}_3: \frac{\partial}{\partial \xi_2} X(\xi_1, 0) = 0, \quad \text{BC}_4: \frac{\partial}{\partial \xi_2} X(\xi_1, 1 + 2\alpha) \\ + \frac{Q}{K} X(\xi_1, 1 + 2\alpha) = 0. \end{aligned} \quad (4.36)$$

The separation of variables technique: $X(\xi_1, \xi_2) = \tilde{X}_1(\xi_1)\tilde{X}_2(\xi_2)$, yields:

$$\left\{ \begin{array}{l} (1/\xi_1)(\xi_1 \tilde{X}'_1(\xi_1))' + \lambda_1 \tilde{X}_1(\xi_1) = 0, \quad \text{for } 0 < \xi_1 < 2 + 1/\alpha, \\ \lim_{\xi_1 \rightarrow 0} \xi_1 \tilde{X}'_1(\xi_1) = 0, \\ \tilde{X}'_1(2 + 1/\alpha) + (Q/K)\tilde{X}_1(2 + 1/\alpha) = 0; \end{array} \right. \quad (4.37)$$

$$\left\{ \begin{array}{l} \tilde{X}_2''(\xi_2) + \lambda_2 \tilde{X}_2(\xi_2) = 0, \quad \text{for } 0 < \xi_2 < 1 + 2\alpha, \\ \tilde{X}'_2(0) = 0, \\ \tilde{X}'_2(1 + 2\alpha) + (Q/K)\tilde{X}_2(1 + 2\alpha) = 0. \end{array} \right. \quad (4.38)$$

Also for this case the eigenvalues $\lambda_{1,n}$ and $\lambda_{2,n}$ are positive: we write, again, $\lambda_{1,n} = \mu_{1,n}^2$ with $\mu_{1,n} > 0$, and $\lambda_{2,n} = \mu_{2,n}^2$ with $\mu_{2,n} > 0$ ($n = 1, 2, 3, \dots$). With the help of the Bessel functions J_0 and J_1 (Abramowitz and Stegun, 1965) we obtain the eigenfunctions:

$$\tilde{X}_{1,n}(\xi_1) = J_0(\mu_{1,n}\xi_1) \quad \text{and} \quad \tilde{X}_{2,n}(\xi_2) = \cos(\mu_{2,n}\xi_2), \quad (4.39)$$

where $\mu_{1,n}$ is the n th positive root of the first and where $\mu_{2,n}$ is the n th positive root of the second of the following two characteristic equations for μ :

$$\begin{aligned} -\mu K J_1(\mu(2 + 1/\alpha)) + Q J_0(\mu(2 + 1/\alpha)) = 0, \\ -\mu K \sin(\mu(1 + 2\alpha)) + Q \cos(\mu(1 + 2\alpha)) = 0. \end{aligned} \quad (4.40)$$

Hence the eigenfunctions $X_{i,j}(\xi_1, \xi_2)$ and corresponding eigenvalues $\lambda_{i,j}$ of the original problem are:

$$X_{i,j}(\xi_1, \xi_2) = J_0(\mu_{1,i}\xi_1) \cos(\mu_{2,j}\xi_2), \quad \text{with} \quad \lambda_{i,j} = \mu_{1,i}^2 + \mu_{2,j}^2. \quad (4.41)$$

The Fourier coefficients $\gamma_{i,j}$ of the constant function $f(\xi_1, \xi_2) = 1$ with respect to this new orthogonal set of eigenfunctions $X_{i,j}(\xi_1, \xi_2)$ follow again from (4.3):

$$\gamma_{i,j} = \frac{\int_0^{2+1/\alpha} \xi_1 \tilde{X}_{1,i}(\xi_1) d\xi_1}{\int_0^{2+1/\alpha} \xi_1 \tilde{X}_{1,i}(\xi_1)^2 d\xi_1} \times \frac{\int_0^{1+2\alpha} \tilde{X}_{2,j}(\xi_2) d\xi_2}{\int_0^{1+2\alpha} \tilde{X}_{2,j}(\xi_2)^2 d\xi_2}, \quad (4.42)$$

which leads, with the shorthand $Q/K = q$, to

$$\begin{aligned} \gamma_{i,j} &= \frac{2q^2}{\mu_{1,i}(2+1/\alpha)(q^2 + \mu_{1,i}^2)J_1(\mu_{1,i}(2+1/\alpha))} \\ &\quad \times \frac{2(-1)^{j+1}q\sqrt{q^2 + \mu_{2,j}^2}}{(1+2\alpha)(\mu_{2,j}^3 + q^2\mu_{2,j}) + q\mu_{2,j}}. \end{aligned} \quad (4.43)$$

The minimum value of (any stationary) $v(\xi_1, \xi_2)$ on a finite cylinder will be found in the centre and the maximum value will be attained on the border circles of the cylinder. In this way we infer from (4.8) and (4.12) for the critical surfaces the following equations:

$$S_{\text{reg}} : \quad K - E = P \sum_{i,j=1}^{\infty} \frac{\gamma_{i,j}}{\mu_{1,i}^2 + \mu_{2,j}^2}, \quad (4.44)$$

$$S_{\text{conf}} : \quad K - E = K(P/E) \sum_{i,j=1}^{\infty} \frac{\gamma_{i,j}J_0(\mu_{1,i}(2+1/\alpha)) \cos(\mu_{2,j}(1+2\alpha))}{P/E + \mu_{1,i}^2 + \mu_{2,j}^2}. \quad (4.45)$$

If we apply to this case the line of reasoning already developed in the last paragraph of Section 4.2.2 we obtain for $\alpha \rightarrow \infty$ the case of an infinite cylinder and for $\alpha \rightarrow 0$ the case of an infinite sheet: an elongated cylinder resembles an infinite cylinder and a flattened cylinder resembles an infinite sheet.

5. CRITICAL SIZE FOR DIFFERENTLY SHAPED ORGANISMS

Due to growth of the organism or to changes in the environmental conditions the organism experiences, the representation $\langle P, Q, E, K \rangle$ of the organism follows a path in parameter space. Also in parameter space we find, subject to the shape of the organism, the critical surfaces S_{reg} and S_{conf} . If the organism changes shape

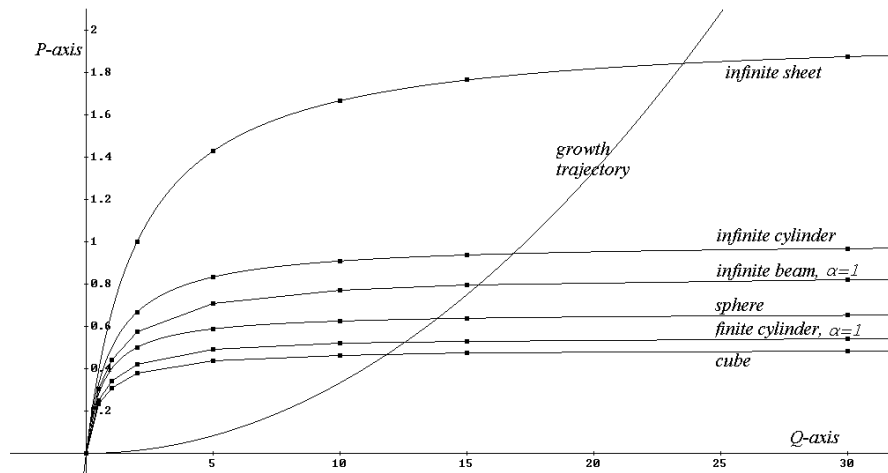


Figure 4. For $E = 0$ and $K = 1$: a parabolic growth trajectory representing undisturbed growth and critical curves for six different shapes. Whenever a growth trajectory crosses a critical curve from below an organism of corresponding shape starts to experience oxygen deficiency.

during its growth process these critical surfaces will shift accordingly in parameter space. A critical point arises whenever the path the organism follows intersects one of its critical surfaces. From a biological point of view the arrival at a critical point is important: we then expect an essential change in the behaviour of the organism.

In this section we discuss what happens at the critical surface S_{reg} for some constant value of E and for $K = 1$. As a result of these restrictions the critical surface S_{reg} degenerates into a critical curve in the reduced parameter space $\langle P, Q \rangle$. In this section we also pay special attention to block-like organisms (block: short for rectangular parallelepiped, see Section 4.2.2). The reason for this is the possibility to distinguish within this class between compact, elongated or flat structures. The numerical justification of the results in this section rests upon equations (3.5), (3.17), (3.25), (4.27), (4.32) and (4.44).

Figure 4 shows, for $E = 0$ and $K = 1$, the critical curves for six organisms of different shape and a possible trajectory an organism, that goes through an otherwise undisturbed growth process, could follow in the reduced parameter space $\langle P, Q \rangle$. During such a growth process only the volume to surface area ratio L of the organism increases, while all other parameter values are constant. In this way we obtain, with the help of equation (2.11), the trajectory $\langle Q(L), P(L) \rangle_L = \langle k_{\text{eff}}L/D, mL^2/(DC_{\infty}) \rangle_L$, which is a simple parabola. An equation for this parabola is: $P = RQ^2$, with $R = P/Q^2 = mD/(k_{\text{eff}}^2C_{\infty})$. Such a parabola is completely determined by the parameter R . The intersection of this parabola with one of the critical curves yields a critical point $(Q_{\text{crit}}, P_{\text{crit}})$. Thus it becomes obvious that the value of Q_{crit} , and therefore the value of L_{crit} , depends solely on the value of the dimensionless parameter combination R (for a given value of E and K and for a given shape of the organism).

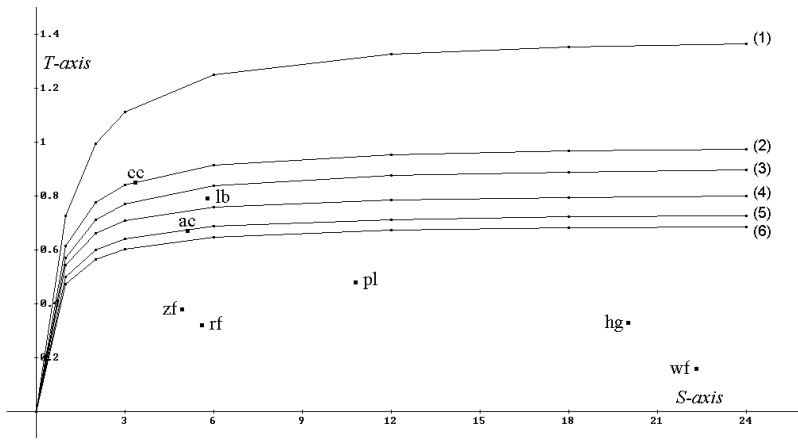


Figure 5. For $E = 0.01$ and $K = 1$; T_{crit} as a function of S for six different shapes: infinite sheet (1), infinite cylinder (2), infinite beam with $\alpha = 1$ (3), sphere (4), finite cylinder with $\alpha = 1$ (5), cube (6). Because $T_{\text{crit}} \propto L_{\text{crit}}$ and $S \propto k_{\text{eff}}$, this picture shows how the outward water conditions influence the critical size of the organism. Also the results for S and T from Table 1 are plotted in this figure: African catfish (ac), common carp (cc), herring (hg), largemouth bass (lb), plaice (pl), rabbitfish (rf), winter flounder (wf), zebrafish (zf).

From Q_{crit} we can deduce L_{crit} [see (2.11)]: $L_{\text{crit}} = DQ_{\text{crit}}/k_{\text{eff}}$. In Fig. 5 we have plotted, for $E = 0.01$ and $K = 1$, the dimensionless parameter $T_{\text{crit}} = Q_{\text{crit}}\sqrt{R}$ as a function of the dimensionless parameter $S = 1/\sqrt{R}$. Because $T_{\text{crit}} = L_{\text{crit}}\sqrt{m/(DC_{\infty})}$ is directly proportional to L_{crit} (and does not depend on k_{eff}) and $S = k_{\text{eff}}\sqrt{C_{\infty}/(mD)}$ is directly proportional to k_{eff} , Fig. 5 shows the dependency of the critical volume to surface area ratio L_{crit} on the mass transfer coefficient k_{eff} . Remember: k_{eff} is a measure for the outward water conditions the organism experiences; the limit $S \rightarrow \infty$ ($k_{\text{eff}} \rightarrow \infty$) represents well-stirred water conditions. Figure 5 also shows that, at least for large k_{eff} , a flattened shape allows for a larger L_{crit} and is therefore more favourable for oxygen supply than a compact one.

In Fig. 5, again, zebrafish, rabbitfish, winter flounder, plaice and herring are smaller than the critical size T_{crit} even for the most disadvantageous shape (i.e., the cube) under the given value of the mass transfer coefficient. This value of the mass transfer coefficient is not large enough to fully meet the oxygen demands of common carp, African catfish and largemouth bass (though note the effect of the shape used to model the embryo).

Next we turn our attention to block-like organisms. A structure from this class is determined by its proportions: $1 : \alpha : \beta$, with $\alpha \geq 1$, $\beta \geq \alpha$ (see Section 4.2.2). This yields a multitude of critical curves $S_{\text{reg}}^{\alpha,\beta}$ in the reduced parameter space $\langle P, Q \rangle$. The positioning of these curves in parameter space is not obvious and is, for instance, quite different for small and large values of Q , see Fig. 6. It can be seen, for instance, that $P_{\text{crit}}^{1,1}(0.05) > P_{\text{crit}}^{10,10}(0.05)$ and $P_{\text{crit}}^{1,1}(2) < P_{\text{crit}}^{10,10}(2)$. Therefore, the critical curves of a cube and a sheet with proportions $1 : 10 : 10$

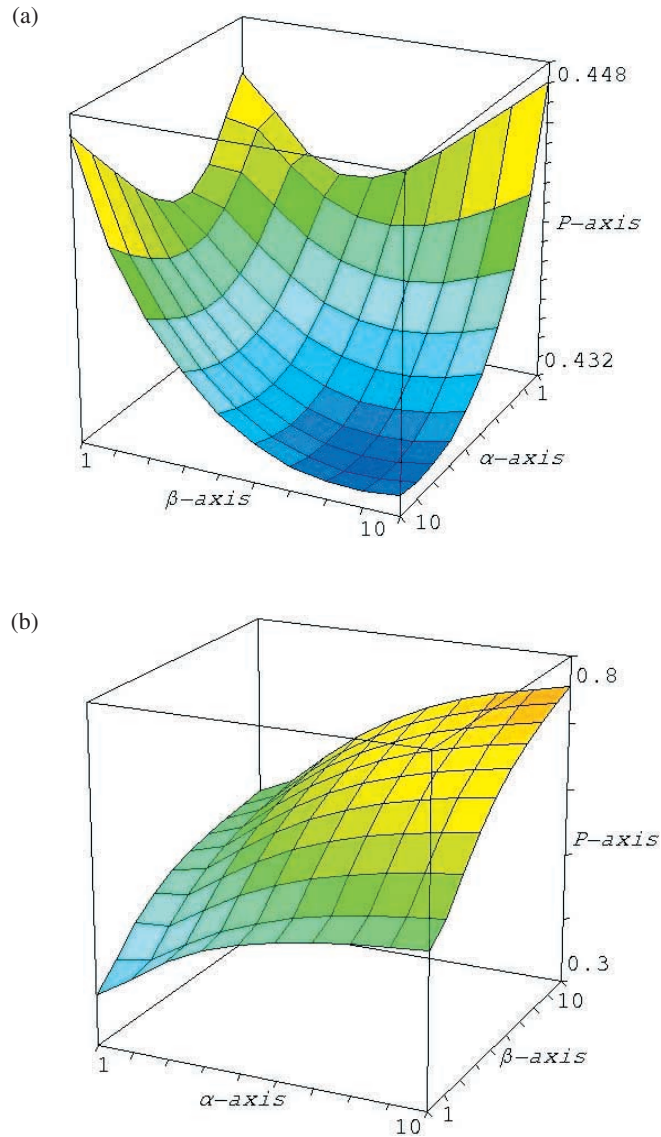


Figure 6. For a block with proportions $1 : \alpha : \beta$ and for $E = 0$, $K = 1$: the critical dimensionless consumption rate P_{crit} as a function of α and β for (a) $Q = 0.05$ and for (b) $Q = 2$. Note the symmetry in α and β : a block with proportions $1 : \alpha : \beta$ behaves the same as a block with proportions $1 : \beta : \alpha$.

coincide somewhere between $Q = 0.05$ and $Q = 2$. Numerical evaluation yields $(Q, P) = (0.0874, 0.072)$ for this common point. It follows that, for conditions compatible with $R = P/Q^2 = 9.425$, a cube and a sheet with proportions $1 : 10 : 10$ share the same value for L_{crit} and hence are equally well equipped for oxygen supply.

As before, we determine for a given value of S (or, equivalently, a given value of R), for all allowed values of α and β , a critical value $Q_{\text{crit}}^{\alpha, \beta}$ (or equivalently $T_{\text{crit}}^{\alpha, \beta}$ or

$L_{\text{crit}}^{\alpha,\beta}$). Using the cube ($\alpha = 1, \beta = 1$) as a gauge, we define the relative critical size $F^{\alpha,\beta}(S)$ by:

$$F^{\alpha,\beta}(S) = \frac{Q_{\text{crit}}^{\alpha,\beta}(S)}{Q_{\text{crit}}^{1,1}(S)} = \frac{T_{\text{crit}}^{\alpha,\beta}(S)}{T_{\text{crit}}^{1,1}(S)} = \frac{L_{\text{crit}}^{\alpha,\beta}(S)}{L_{\text{crit}}^{1,1}(S)}. \quad (5.1)$$

Hence, if it holds for a given value of S that $F^{\alpha,\beta}(S) < 1$, then the critical size of a block-like organism with proportions $1 : \alpha : \beta$ is smaller than the critical size of a cube, which means that a cube for the given value of S is more favourable for oxygen supply.

In Fig. 7(a) we have plotted $F^{\alpha,\beta}$ for a small value of S (i.e., a small value of k_{eff}) and in Fig. 7(b) we have plotted $F^{\alpha,\beta}$ for a large value of S (i.e., a large value of k_{eff}). The results show that for almost stagnant water a compact structure is more favourable for oxygen supply and that for well-stirred water conditions a flat shape is more favourable. This concurs with the predictions already made by Kranenborg *et al.* (2001).

Apart from pure growth an organism may also (slowly) change its shape. During such a process, supposing all other parameter values are kept constant, again only the volume to surface area ratio L of the organism changes. Hence the organism follows again a parabola in parameter space. In addition the change of shape of the organism also results in a new corresponding critical curve.

If we take, for instance, a block-like organism with proportions $1 : \alpha_0 : \beta_0$, with volume V_0 and with volume to surface area ratio L_0 , we have:

$$V_0 = \frac{(\alpha_0 + \beta_0 + \alpha_0\beta_0)^3}{\alpha_0^2\beta_0^2} 8L_0^3. \quad (5.2)$$

Hence, if a block with proportions $1 : \alpha_0 : \beta_0$ and with volume to surface area ratio L_0 alters into a block with proportions $1 : \alpha_1 : \beta_1$ and with volume to surface area ratio L_1 , at the same time changing its volume V_0 into $V_1 = g^3 V_0$, we have:

$$L_1 = \frac{\alpha_0 + \beta_0 + \alpha_0\beta_0}{\alpha_1 + \beta_1 + \alpha_1\beta_1} \left(\frac{\alpha_1\beta_1}{\alpha_0\beta_0} \right)^{2/3} g L_0. \quad (5.3)$$

By comparing, for a given value of S , L_0 with $L_{\text{crit}}^{\alpha_0,\beta_0}(S)$ and L_1 with $L_{\text{crit}}^{\alpha_1,\beta_1}(S)$ it is possible to see if the proposed growth-spurt of the organism will result in a change of its oxygen consumption pattern and, therefore, of its behaviour. Following this procedure it can be shown, for example, that a critical cube would change into a supercritical sphere if the volume were kept constant in the transition.

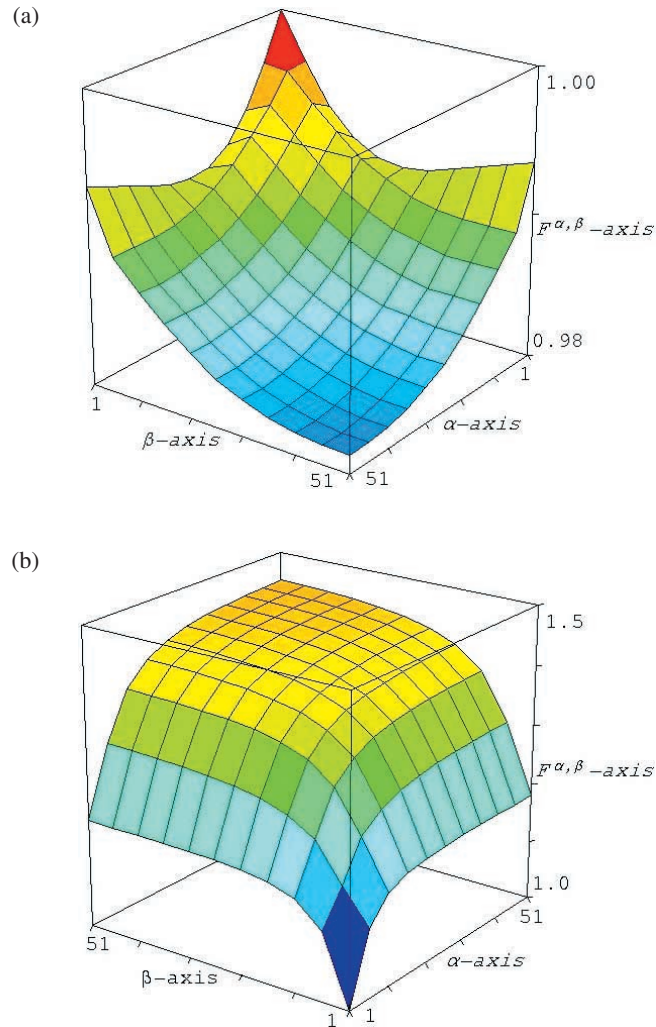


Figure 7. For a block with proportions $1 : \alpha : \beta$ and for $E = 0, K = 1$: the relative critical size $F^{\alpha, \beta}(S)$ as a function of α and β for (a) $S = 0.05$ (a cube appears to be the most favourable shape for oxygen supply) and for (b) $S = 1$ (a cube appears to be the least favourable shape for oxygen supply).

6. DISCUSSION

We presented a model that describes the oxygen balance in small organisms without an active internal oxygen transport mechanism, e.g., flatworms (*Platyhelminthes*) or precirculation embryos of higher organisms. In three important aspects this model expands on earlier models of oxygen transport. Firstly, we included the effect of a moving medium on the oxygen balance. Secondly, we modelled the consumption pattern of the organism as a combination of regulator behaviour above a specified threshold oxygen concentration and conformer

behaviour below the threshold. This is a more realistic oxygen consumption pattern than a pure regulator or a pure conformer pattern as adopted in previous models. And thirdly, by using the method of eigenfunction expansion we were able to treat, within our model, organisms with a wide variety of shapes, contrary to existing analytical models that mainly analyse infinite sheets, infinite cylinders or spheres.

We defined four dimensionless parameters that completely describe the state of the organism. This state includes the value of tissue variables (oxygen diffusion coefficient, maximum respiration rate, oxygen consumption concentration threshold), outward conditions variables (mass transfer coefficient, free water oxygen concentration), and size and shape of the organism. For a given shape of the organism, and based on the oxygen concentration threshold, we were able to define the critical surfaces S_{reg} and S_{conf} . These surfaces divide parameter space into three domains: the regulator domain (oxygen deficiency nowhere in the organism), the mixed domain (oxygen deficiency at least somewhere in the organism), and the conformer domain (oxygen deficiency everywhere in the organism). Oxygen deficiency is defined here as a local oxygen concentration below the threshold concentration.

A change in the four parameters describing the state of the organism may, for instance, occur due to a variation in environmental conditions (for instance, a change of the ambient temperature) or due to growth of the organism. Such a change triggers a journey along a certain trajectory in parameter space. Whenever this trajectory crosses a critical surface in parameter space, an essential change in the behaviour of the organism is expected. If, for example, such a trajectory enters the conformer domain (i.e., passes S_{conf}), the organism experiences oxygen deficiency everywhere in its tissues and lowers its respiration rate. Eventually, this may lead to the complete shut down of certain biological processes, cf. the suspended animation observed in zebrafish embryos after they had been transferred to an anoxic environment (Padilla and Roth, 2001).

If a trajectory in parameter space enters the mixed domain from the regulator domain (i.e., passes S_{reg}), this marks the onset of oxygen shortage somewhere in the organism. Because oxygen is needed to perform essential biological processes such as aerobic respiration and growth, we expect natural selection to favour residence of an organism without a circulatory system in the regulator domain. This enabled us to define a critical size for an organism: the largest size for which it can maintain pure regulator behaviour. Size is defined here as the volume to surface area ratio, so the critical size represents the maximum volume of respiring tissue that can be fully supplied with oxygen per unit surface area.

The shape of an organism, apart from its size, acts in our model as a 'fifth' independent variable. Contrary to the prevailing models of oxygen supply to small organism, this feature of our model enabled us to analyse the class of block-like organisms. In fact, even more exotically shaped organisms can be analysed, though this would require numerical methods, such as Galerkin procedures. The analysis of the class of block-like structures allowed us to distinguish between cube-like,

elongated and sheet-like organisms. In this way we were able to confirm a conjecture of Kranenborg *et al.* (2001): they stated that for almost stagnant water a flat shape is more favourable for oxygen supply, while for well-stirred water conditions a compact shape is more favourable.

The analysis of oxygen dynamics data of teleost embryos from Kranenborg *et al.* (2000) illustrates a useful application of the presented theoretical framework. Several teleost embryos (zebrafish, rabbitfish, winter flounder, plaice and herring) appear to be relatively insensitive to external flow conditions. These species will not experience oxygen deficiency even in nearly stagnant water. Other species however (common carp, African catfish and largemouth bass) apparently need a certain amount of external stirring to fully meet their oxygen demands.

Oxygen consumption data of common carp and African catfish are considerably higher than the average oxygen consumption of teleost embryos (Kranenborg *et al.*, 2000). This could be indicative of rearing conditions with excess oxygen. The predictions for maximum size for these specimens should therefore be interpreted with caution.

Interestingly, largemouth bass is the only species in our analysis in which the male fans the nest in which the eggs are deposited (Scott and Crossman, 1973). This fanning greatly enhances external stirring and might explain the relatively large size of the largemouth bass embryo.

REFERENCES

- Abramowitz, M. and I. A. Stegun (Eds) (1965). *Handbook of Mathematical Functions*, New York: Dover.
- Byatt-Smith, J. G., H. J. Leese and R. G. Gosden (1991). An investigation by mathematical modelling of whether mouse and human preimplantation embryos in static culture can satisfy their demands for oxygen by diffusion. *Hum. Reprod.* **6**, 52–57.
- Carslaw, H. S. and J. C. Jaeger (1959). *Conduction of Heat in Solids*, 2nd edn, New York: Oxford University Press.
- Churchill, R. V. (1955). Extensions of operational mathematics, *Proc. Conf. Diff. Eqns.*, University of Maryland.
- Clift, R., J. R. Grace and M. E. Weber (1978). *Bubbles, Drops, and Particles*, New York: Academic Press.
- Daykin, P. N. (1965). Application of mass transfer theory to the problem of respiration of fish eggs. *J. Fish. Res. Bd Can.* **22**, 159–171.
- Desaulniers, N., T. S. Moerland and B. D. Sidell (1996). High lipid content enhances the rate of oxygen diffusion through fish skeletal muscle. *Am. J. Physiol.* **271**, R42–R47.
- Dowse, H. B., S. Norton and B. D. Sidell (2000). The estimation of the diffusion constant and solubility of O₂ in tissue using kinetics. *J. Theor. Biol.* **207**, 531–541.
- Fairweather, G. (1978). *Finite Element Galerkin Methods for Differential Equations*, New York: Dekker.

- Fenn, W. O. (1927). The oxygen consumption of frog nerve during stimulation. *J. Gen. Physiol.* **10**, 767–779.
- Gerard, R. W. (1931). Oxygen diffusion into cells. *Biol. Bull.* **60**, 245–268.
- Gielen, J. L. W. (2000). The general packed column: an analytical solution. *IMA J. Appl. Math.* **65**, 123–146.
- Graham, J. B. (1988). Ecological and evolutionary aspects of integumentary respiration: body size, diffusion and the Invertebrata. *Am. Zool.* **28**, 1031–1045.
- Harvey, E. N. (1928). The oxygen consumption of luminous bacteria. *J. Gen. Physiol.* **11**, 469–475.
- Kranenbarg, S., M. Muller, J. L. W. Gielen and J. H. G. Verhagen (2000). Physical constraints on body size in teleost embryos. *J. Theor. Biol.* **204**, 113–133.
- Kranenbarg, S., J. H. G. Verhagen, M. Muller and J. L. Van Leeuwen (2001). Consequences of forced convection for the constraints on size and shape in embryos. *J. Theor. Biol.* **212**, 521–533.
- Krogh, A. (1919). The rate of diffusion of gases through animal tissues, with some remarks on the coefficient of invasion. *J. Physiol. Lond.* **52**, 391–408.
- Krogh, A. (1941). *The Comparative Physiology of Respiratory Mechanisms*. Philadelphia, PA: University of Pennsylvania Press.
- Lee, C. E. and R. R. Strathmann (1998). Scaling of gelatinous clutches: effects of siblings competition for oxygen on clutch size and parental investment per offspring. *Am. Nat.* **151**, 293–310.
- Longmuir, I. S. (1957). Respiration rate of rat-liver cells at low oxygen concentrations. *Biochem. J.* **65**, 378–382.
- Padilla, P. A. and M. B. Roth (2001). Oxygen deprivation causes suspended animation in the zebrafish embryo. *PNAS* **98**, 7331–7335.
- Rosen, J. B. (1952). Kinetics of a fixed bed system for solid diffusion into spherical particles. *J. Chem. Phys.* **20**, 387–394.
- Scott, W. B. and E. J. Crossman (1973). *Freshwater Fishes of Canada*. Ottawa: Fisheries Research Board of Canada, Bulletin 184.
- Seymour, R. S. and D. F. Bradford (1987). Gas exchange through the jelly capsule of the terrestrial eggs of the frog, *Pseudophryne bitroni*. *J. Comp. Physiol. B* **157**, 477–481.
- Strathmann, P. R. and C. Chaffee (1984). Constraints on egg masses. II. Effects of spacing, size, and number of eggs on ventilation of masses of embryos in jelly, adherent groups, or thin-walled capsules. *J. Exp. Mar. Biol. Ecol.* **84**, 85–93.
- Warburg, O. (1923). Versuche an überlebendem carcinoomgewebe. [Methoden]. *Biochem. Z.* **142**, 317–333.
- Wickett, W. P. (1975). Mass transfer theory and the culture of fish eggs, in *Chemistry and Physics of Aqueous Solutions*, W. A. Adams, G. Greer, J. E. Desnoyers, G. Atkinson, G. S. Kell, K. B. Oldham and J. Walkley (Eds), Princeton: The Electrochemical Society, Inc., pp. 419–434.